Sixth International Symposium on Marine Propulsors
smp'19, Rome, Italy, May 2019

Development of Tunnel Thruster Series Propellers for Low Noise and Vibration

Jie Dang[1] and Do Ligtelijn[2]

[1]Maritime Research Institute Netherlands (MARIN), Wageningen, The Netherlands
[2]Retired, Maritime Research Institute Netherlands (MARIN), Wageningen, The Netherlands

ABSTRACT

Since the systematic study carried out more than 50 years ago by Taniguchi et al. (1966), not so much effort has been made to tunnel thrusters with regard to the propeller blade design and the thruster hydrodynamic performance. In addition to a lack of information on the influences of tunnel form, entrance shape, grid bars and ship hull inclination on the side force performance, very limited information is available in the public domain on noise and vibration levels of a tunnel thruster in operation.

In order to assist the industry to meet the higher demands on comfort class of a ship at present days, the Maritime Research Institute Netherlands (MARIN) initiated 3 years ago a Joint Industry Project (JIP) on tunnel thrusters, focusing on noise and vibrations as well as the side force. A joint investment has been made by 23 industry partners and MARIN, together with Dutch government subsidies. The study has been going for 3 years since then, through investigations on low noise and vibration thruster designs, series propeller designs, model tests, data acquisition and analyses, results reporting and software development, and finalized at the end of 2018.

The study covers the effects of tunnel length (2.5 to 12.0 times tunnel diameter), ship hull inclination (90^o to 65^o vertically and horizontally), tunnel opening's forms (chamfered, round, sharp and double-chamfered), grid bars (5 to 9 flat) for both conventional mechanical gear-driven fixed pitch and controllable pitch propellers as well as rim-driven propellers with various number of blades (4 to 7), blade area ratios (0.45 to 0.90) and pitch ratios (0.65 to 1.15). The propeller design methodology was also investigated with respect to the main parameters, such as the effects of the skew (forward and backward), the blade contour, the pitch distribution, as well as the s-shaped camber form for fixed pitch tunnel propeller blades. The study includes the effects of those parameters on the side force, the cavitation performance, the pressure pulse levels, the excitation forces on the tunnel segment and the underwater radiated noise levels in the far field.

The project accumulated huge amounts of data, enormous experience and test results. Selected information is made available in the present paper.

Keywords

Side thruster, Tunnel thruster, Cavitation, Noise, Vibration.

1 INTRODUCTION

Lateral thrusters, also called side thrusters or tunnel thrusters (TTs) installed at the bow or stern of a ship, were widely used since the 1960's for assisting ship's low speed maneuvering operations, such as for train ferries, car ferries and other ships like buoy-tenders, etc. Typically, such a system consists of a right-gearbox in a tunnel through the ship's body from one side to the other, fitted with fixed pitch propellers (FPPs) with constant pitch or with controllable pitch propellers (CPPs) with planar blades set to various pitches in operations.

After the pioneer work conducted by Pehrsson (1960) on the hydrodynamic performance of a TT by using a ship segment model fitted with CPP blades, and the early findings of English (1963) on the significant performance losses of a TT with ship speed, the most complete and comprehensive studies on a tunnel thruster were carried out by Taniguchi et al. (1966). Since then their work has formed the basis for the tunnel thruster designs and for the operation estimations for more than 50 years, used as the guidelines until now.

Taniguchi's studies consist of systematic studies of the TT in which the propeller geometry has been varied as well as the tunnel geometry (the length, the inlet shapes, the grid bars, the wall inclinations, the shaft immersion, the bottom height, etc.); the lateral force tests of typical ships at various ship speeds with wall and bottom effects; the resistance increases due to tunnel openings; the maneuvering tests of course changing, turning, quay approaching and leaving, etc. It is noted that in that work the aspects of noise and vibrations could not be considered. Also, no gearbox housing model was present in the experiments, so that there was no difference in performance between operating to portside or starboard side.

Useful summaries of the work done in the 1960's can be found in Beveridge (1971), Pronk and Schneiders (1976), Verbeek (1982), and Carlton (2007), enriched further by studies of Chislett and Björheden (1966) on the ship speed influences, Brix and Bussemaker (1973) on the anti-suction tunnels, Kijima (1977) on ship's drift angle effects, Buiten & Regt (1973) and Ligtelijn & Otto (2013) on noise and vibrations, etc.

Tunnel thrusters have found even wider applications in recent years, from cruise ships with high powered thrusters (over 5MW per unit) to dredgers with very long tunnels (more than 10 times of the tunnel diameter), from dynamic positioning operations for offshore vessels such as a floatel where silent operation of the systems is essential during crew's sleeping, to crabbing operation of ferries in severe weather without assistance of tug boats. However, the hydrodynamic study of tunnel thrusters, especially with increased strict requirements on their vibration and noise levels, is lagging behind. There are even no tunnel thruster series (TT-series) propellers available for the industry for early design stage selection and performance estimations, neither for FPPs in tunnels (FTTs) nor CPPs in tunnels (CTTs). Furthermore, and in the mean time, new types of lateral thrusters have been invented to meet the electrification of the industry and even higher demands on vibration and noise, such as rim-driven fixed pitch propellers in a tunnel as side thrusters (RFTTs).

In order to assist the industry on tunnel thruster design and operation, and by joined investment of the industries and the Dutch government through subsidies, a Joint Industry Project (JIP) was formed 3 years ago on developing tunnel thruster series propellers for CTTs, FTTs and RFTTs, with focus on reducing vibration and noise levels, called the Wageningen TT-Series JIP. In this JIP, some of the investigations in the early years have been re-visited; various blade design strategies have been studied; the tunnel vertical and horizontal excitation forces and the pressure fluctuations on the tunnel surface have been measured; and the underwater radiated noise (URN) levels have been established systematically, which have been lacking so far in the public domain.

In the meantime, Computational Fluid Dynamics (CFD) has found wide application in both performance analysis as well as tailor-made TT thruster blade design, see an early CFD study by Nienhuis (1992) and more recently by Funeno (2006) and Mohan (2017). The Wageningen TT-Series JIP provides a database for the CFD validation.

In the present paper, the Wageningen TT-series is described, the model test set-ups and the test procedures have been given. Selected initial test results are presented, released with approval of all JIP participants, followed by discussions on the blade design strategies and the test results.

2 THE WAGENINGEN TT-SERIES AND MODELS

The Wageningen TT-series propellers consists of 3 CTTs, 24 FTTs and 9 RFTTs in total, with various blade numbers (Z), blade area ratios (BAR) and blade pitch ratio's (P/D_P) where D_P is the propeller diameter. In addition, 12 propeller models with different design strategies have been manufactured and tested in the early investigations on the blade design strategy. Not all series have a full matrix of propeller models, but crosses in the space of Z, BAR and P/D_P for practical reasons. Table 1 provides an overview of the whole series.

Table 1 The Wageningen TT-Series Propellers

Design P/D_P	BAR			
	0.45	0.60	0.75	0.90
0.0	CTT4-45	CTT4-60	CTT4-75	–
0.65	FTT4-45	FTT4-60	FTT4-75	FTT4-90
0.90	FTT4-45	FTT4-60	FTT4-75	FTT4-90
1.15	FTT4-45	FTT4-60	FTT4-75	FTT4-90
0.65	–	FTT5-60	FTT5-75	FTT5-90
0.90	–	FTT5-60	FTT5-75	FTT5-90
1.15	–	FTT5-60	FTT5-75	FTT5-90
0.65	–	–	FTT7-75	–
0.90	–	–	FTT7-75	–
1.15	–	–	FTT7-75	–
0.90	–	–	RFTT4-75	–
0.65	–	–	RFTT5-75	–
0.90	–	RFTT5-60	RFTT5-75	RFTT5-90
1.15	–	–	RFTT5-75	–
0.65	–	–	RFTT7-75	–
0.90	–	–	RFTT7-75	–
1.15	–	–	RFTT7-75	–

Although the CTTs have planar blade designs at zero pitch ratio, they were set to various pitch ratios at P/D_P = 0.00, ±0.50, ±0.65, ±0.90, and ±1.15, during their performance study.

The blade design addressed in the present study accounts for tunnel thrusters used in generating side forces in both directions (to port side as well as to starboard side) by either changing the rotating direction of the FTTs and RFTTs or the pitch from positive to negative while keeping the same rotation direction for the CTTs. Therefore, all CTTs have planar blades and all FTTs and RFTTs have identical nose and tail form of the section profile with zero mean camber and without rake or skew. Dedicated TT designs optimized for only one operation direction are not included in the present series.

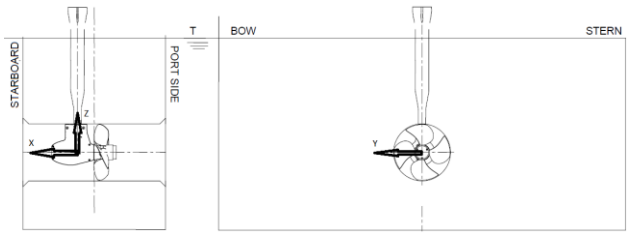

(a) gear-driven system

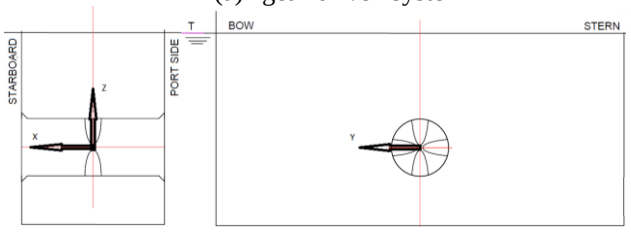

(b) rim-driven system

Figure 1 The basic ship segment models for the tests.

The whole series has been tested using the basic ship segment models as shown in Figure 1 with a tunnel length of $2.5D_T$ and a shaft height from the baseline of $1.35D_T$ with 45^o chamfered edges of the opening with a width of 10% D_T, with a tunnel model diameter D_T of 21 cm,

envisaging a 2.1 m tunnel in full scale (scale ratio 1:10). The coordinate systems shown in Figure 1 are defined according to the thruster manufacturer's preferences.

For the gear-drive system, the propeller tip clearance is 0.7%D_T so that the propeller diameter D_P is 1.4% smaller than the tunnel inner diameter D_T with a pod diameter of 44.4% D_T. For the rim-drive system, $D_P = D_T$.

It is already known that the ship's hull form, the tunnel and the opening details have strong influences on the TT performance, with regard to not only the side force, but also the cavitation, vibration, and noise levels. Therefore, selected propellers have also been tested in various ship's segment models, that include:

Tunnel length of 2.5 D_T, 4.0 D_T, 8.0 D_T and 12.0 D_T.

Wall inclinations vertical (90°), 75°, 65°, and combined vertical and horizontal inclination at 75°, see Figure 2.

Tunnel entrance form of '45°-chamfered', 'round', 'sharp' and 'double-chamfered', see also Figure 2.

Entrance grid bars with 'flat-round' as, coarse: 5-2, normal: 7-2 and fine: 9-2, with identical blockage and total wetted surface, see Figure 3.

Gearbox pod support: I- and V-supports, see Figure 4.

Interpolation of those test results provides complete information on the side force, cavitation, pressure fluctuations, tunnel excitation forces and noise levels for the whole series with the influence of the geometry details mentioned above.

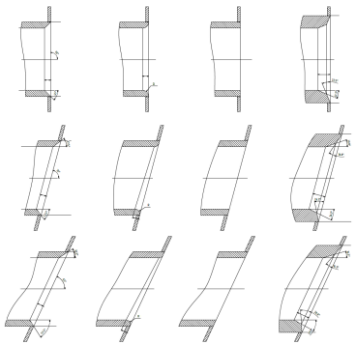

Figure 2 Wall and entrance, left-right: chamfered, round, sharp, double-chamfered; top-bottom: wall 90°, 75°, 65°.

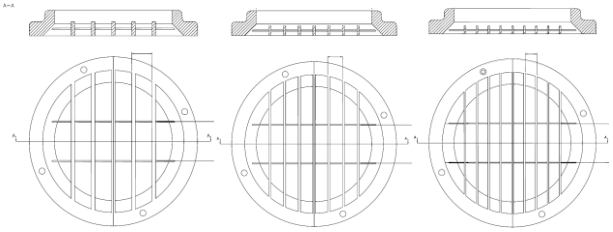

Figure 3 The grid bars, left to right: 'coarse', 'normal', and 'fine'.

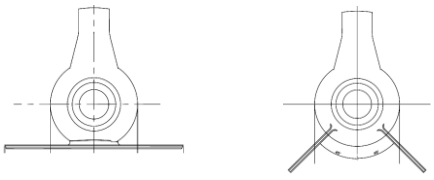

Figure 4 I-support and V-support for the gearbox pod.

3 TEST SET-UPS AND INSTRUMENTATION

Two basic test set-up drives have been built, one with a generic gearbox pod of mechanical driven system with carefully designed and manufactured gears for low mechanical noise and vibrations, see Dang et al. (2013), and the other with a rim-driven system, Klinkenberg et al. (2017). See the photo's in Figure 5 for both drives.

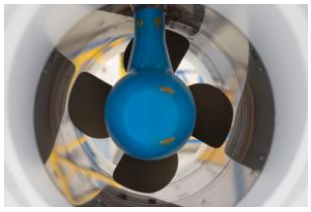

Figure 5 The gear-driven (l) and rim-driven (r) systems.

Multiple six-component force transducers or frames (6Cs) have been used to record the force loads on various parts of the systems.

In the gear-driven system, the following 6Cs were used:

A shaft 6C connected to one key blade of the CTT propellers to measure both mean and also dynamic loads up to 500Hz in model scale, see Dang et al. (2014, 2015), and the total propeller thrust and torque to be composed from the blade loads. The shaft thrust and torque transducers, used when spindle torque or dynamic blade loads were less important, like for FTTs, were of the conventional type.

A 6C frame to measure the total pod thrust, bending moments, steering moment among others. The difference between the propeller thrust and the pod thrust is seen as the drag of the gearbox pod.

A large 6C frame connects the ship segment models to the towing carriage of the tank to measure the mean total side force on the hull, see the installation drawings in Figure 7 on the next page.

For the rim-driven system, the thrust and torque of the ring-propellers were measured by in-house made ring-shaped transducers between the propeller ring, on which the blades were fitted, and a driving ring with a larger diameter driven through a low noise V-belt by electric motors in the ship's segment model.

In order to record the tunnel excitation forces, a special ring-shaped 6C frame has been built with the highest possible stiffness while sensitive enough to capture the dynamic fluctuations on a tunnel segment, which has the lowest possible mass density (Perspex) so that its natural frequency, taken into account the added mass effects, is high enough, see Figure 6. Therefore, the blade frequency component can be well measured, with hopes that the higher harmonics can be also indicative.

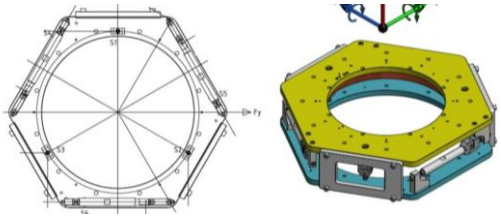

Figure 6 6C frame on tunnel segment for excitation force.

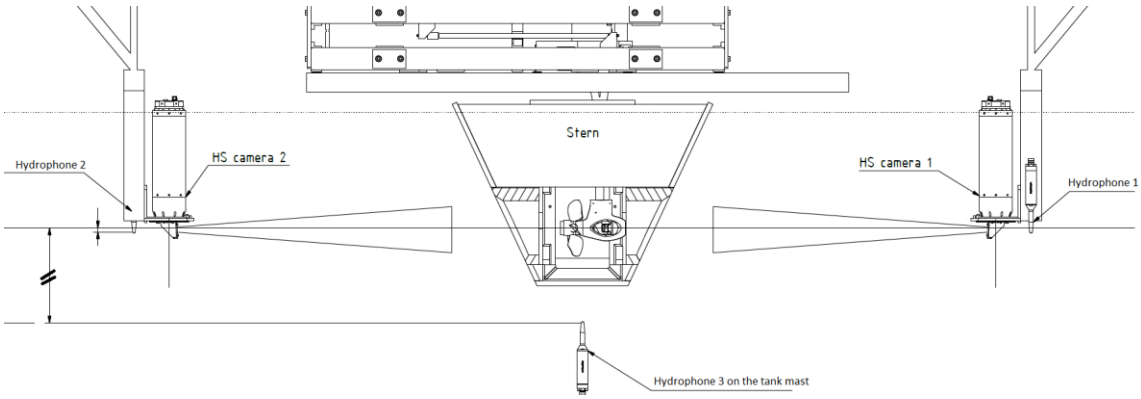

Figure 7 Illustration of one ship segment model connected to the towing carriage through a large 6C load frame in MARIN's Depressurized Wave Basin (DWB) with hydrophones and high speed (HS) video cameras installed.

To measure the pressure fluctuations on the tunnel wall, 30 pressure transducers have been installed on the tunnel segment in way of the propeller tips for the gear-driven system and 9 pressure transducers have been installed on the segment tunnel on one side of the ring-propeller for the rim-driven system, assuming perfect symmetry for the rim-driven system. The distribution of transducers are shown in Figure 8.

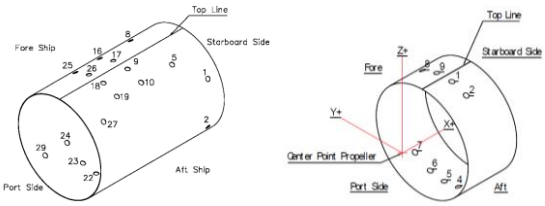

Figure 8 Distribution of pressure transducers on the tunnel segments of the gear-driven system (left) and the rim-driven system (right).

Three hydrophones were used to record the underwater radiated noise (URN) levels with two facing both tunnel openings (hydrophone 1 and 2 in Figure 7) and one fitted to the mast from the tank bottom, measuring beneath the ship segment model (hydrophone 3 in Figure 7). The hydrophones were placed at a distance such that the noise levels can be measured as far-field noise levels however without much dissipation and reflection of the tank walls and bottom. The ship segment models are made of wood and the tunnels are made of Perspex so that the test set-ups are built as much possible transparent for sound, while the segment models are always filled with water. With the system calibrated by a standard noise source, transfer functions for the test set-up could be determined.

Four high speed (HS) video cameras were used to observe the cavitation patterns on any part of the test set-up, mainly for the propeller blades. Two of them were installed next to the hydrophone 1 and 2 as shown in Figure 7 looking at the suction side or pressure side of the propeller blades, depending on the rotation direction of FTTs and RFTTs or the pitch setting of the CTTs. In addition, two HS video cameras were located in the ship segment model looking through the transparent Perspex tunnel segment at the gaps of propeller tips, recording the tip cavitating flow, see Figure 9.

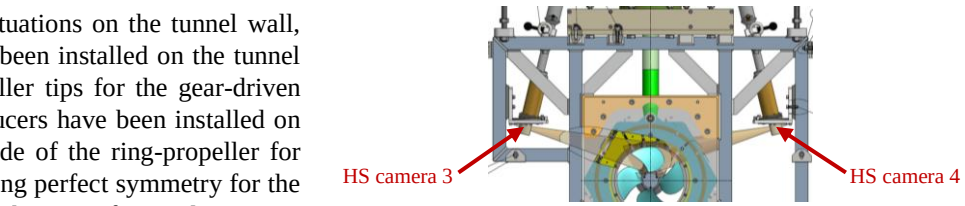

Figure 9 Two HS video cameras looking at the tip gap of the propeller blades for the gear-driven system.

For high speed video recordings, strong illumination is needed. This was achieved by using many LED light strips distributed in the ship segment models which were painted white inside, see Figure 10 as an example.

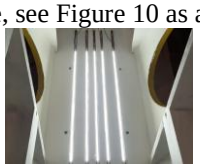

Figure 10 LED Illumination for HS video recordings.

Turbulent flow through the tunnel was stimulated by roughness strips of 60 μm at the openings, as shown on the photo in Figure 11. Also applied were electrolysis wires at both entrance on the hull surface but very close to the tunnel openings to generate enough nuclei into the tunnel where the propeller was operating and the ship segment model was standing still. The nuclei are important for cavitation inception, especially for the gap and vortex flows around the blade tip region.

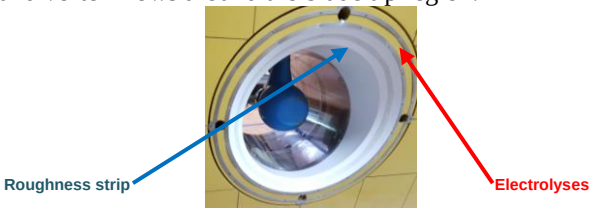

Figure 11 Turbulence stimulation and nuclei generation at the openings, the gear-drive without blade as an example.

Different from the normal propeller cavitation test procedure at MARIN, no roughness along the leading edge of the propeller blades has been applied. Due to the nature of the tunnel thruster propeller blades with zero camber to ensure equal operation in both operation directions, sharp and high suction peaks at the leading edge of the blades are expected, resulting in natural transition from laminar to turbulent flow.

4 DATA ACQUISITION, REDUCTION AND ANALYSIS

It was a great challenge to record loads from multiple 6C transducers, pressure fluctuations from 30 pressure transducers, noise levels from 3 hydrophones, high speed videos from 4 HS cameras, together with operational and environmental conditions of the tank, simultaneously. In addition, all recordings were synchronized.

The following is a photo showing how complex the system is that must function well in vacuum conditions.

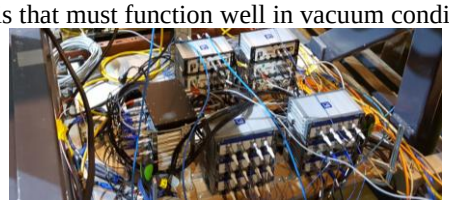

Figure 12 Example of the data acquisition systems.

All signals from the 6C transducers were sampled at 1,200 Hz to obtain the mean loads. In order to record dynamic loads on the propeller shaft on the key blades and also the vertical and horizontal excitations of the tunnel segment up to as high as the 4th blade passing frequency, a 9,600 Hz sampling frequency was used.

Although the hydrophones have a very wide range on the response frequency, the noise levels measured in the low frequency range represent mainly the model noise levels, including also the noise from the drives and the resonance of the test set-up and carriage itself. The only meaningful URN levels measured are the cavitation noise levels in the high frequency range. The sampling frequencies used during the model tests were high, covering a range starting from 88Hz to 100kHz.

The measured 6C loads were further filtered, reduced and processed into mean values as well as dynamic amplitudes represented by 95% occurrence intervals, see Dang and Brouwer (2014, 2015). Since only the natural frequency on the key blade is very high (>500Hz), the hydrodynamic loads are well measured with high resolution in one single rotation of the blade, but the measured dynamic loads on the gearbox pod and the total ship side force were only for indication.

The details regarding the noise measurements, calibration, the way to determine the transfer functions are provided in Klinkenberg et al. (2017).

5 TYPE OF TESTS

All tests were carried out at MARIN's Depressurized Wave Basin (DWB), measuring 240x18x8 m. The segment models were located about half way the length of the tank, the tunnel axis coinciding with the tank centerline. In this way the segment models can be tested at zero speed (bollard) condition without flow blockage and circulation effects, while at reduced air pressure for cavitation simulations. A description of the DWB can be found in various publications, such as Dang (2014).

To capture all performance aspects of a tunnel thruster and to limit the possible scale effects, the following tests have been carried out for the Wageningen TT-Series Propellers at zero ship speed:

Run-up tests of the rotational rates from 500 RPM to 1,500 RPM with a step of 200 RPM, additional runs at 1,000 RPM for the gear-driven system to avoid resonance.

Sweep tests with rotational rate varying between 500 RPM and 1,500 RPM at 3 tank air pressure levels in order to obtain the thrust breakdown curve with respect to the cavitation number, defined below.

Dedicated cavitation observations, tunnel pressure fluctuation measurements, tunnel vertical and horizontal excitation forces, URN levels measurements, and static and dynamic loads measurements at 1,000 RPM in bollard condition for 3 cavitation numbers of 1.5, 2.0 and 2.5 on the tunnel center line (shaft line) in the normal tunnel thruster operation range. All test results, observations and recordings were synchronized.

To obtain purely the hydrodynamic performance, all model mechanical, structural, electronic, environmental influences, etc. were removed, reduced or restricted by calibrations, zeroing, sheltering and/or additional tests, such as the tests in air to subtract the centrifugal forces on the blades, the background noise and noise transfer function measurements to judge the validity of the measured noise and to determine the noise source levels.

Measured URN levels were only considered directly valid when they were at least 10dB higher than that of the background noise levels measured with the drive systems operating without blades. The measured URN levels between 3 to 10 dB were corrected and those lower than 3 dB were discarded.

For all tests, the rotational cavitation number σ_n is defined as,

$$\sigma_n = \frac{P_0 + \rho g h - P_v}{0.5 \rho n^2 D_P{}^2}, \tag{1}$$

where P_0 is the tank pressure, P_v is the vapor pressure, h is the tunnel center line immersion or shaft immersion and n is the rotation rate. All 6C loads measured were non-dimensionalised into coefficients,

$$K_{Fx} = \frac{F_x}{\rho n^2 D_P{}^4}; K_{Fy} = \frac{F_y}{\rho n^2 D_P{}^4}; K_{Fz} = \frac{F_z}{\rho n^2 D_P{}^4}, \tag{2}$$

$$K_{Mx} = \frac{M_x}{\rho n^2 D_P{}^5}; K_{My} = \frac{M_y}{\rho n^2 D_P{}^5}; K_{Mz} = \frac{M_z}{\rho n^2 D_P{}^5}, \tag{3}$$

where F_x and M_x are propeller thrust T and torque Q.

To judge the efficiency of generating the side force, a merit coefficient η_D defined on the total hull side force coefficient K_{Fx_hull} and propeller torque coefficient K_Q has been used,

$$\eta_D = \frac{\left(\left|K_{Fx\_hull}\right|/\pi\right)^{3/2}}{\left|K_Q\right|}. \tag{4}$$

The measured noise levels are presented in dB values in 1/3-octave band and converted to 1 m distance to the source and based on a reference pressure of 10^{-6} Pascal.

6 RESULTS AND DISCUSSION

It is impossible to publish the whole set of data from the Wageningen TT-Series Propellers in one paper. Therefore, only selected data and findings in the initial investigations on the blade design strategy are provided and discussed below.

It was intended to investigate thrusters as much as possible in a practical tunnel- and hull form and to investigate various blade forms to assess the design strategy for a practical application. A segment ship model with 65° wall inclination and 45° chamfered edges without grid bars has been selected for the initial investigations, see the photo in Figure 13. 12 propeller models with various blade design have been tested.

Figure 13 Ship segment model used in the initial tests.

6.1 Cavitation patterns

The same as for a main propulsion system where a ship's wake field has the strongest influence on the cavitation performance of the propeller, the cavitation on the blades of a TT propeller is also greatly affected by the flow in the tunnel which depends strongly on the hull- and tunnel form, the entrance details and the gearbox. To illustrate this, Figure 14 shows two HS video screenshots on one very conventional 4-bladed CTT propeller and on one 7-bladed RFTT propeller with advanced design.

Figure 14 Cavitation patterns on CTT1 (Kaplan, 4-bladed, $P_{0.7R}/D_P$=0.9, BAR=0.6) and RFTT2 (7-bladed, $P_{0.7R}/D_P$= 0.9167, BAR=0.6), σ_n=2.5 at bollard, rotation CCW.

It is clearly seen that the largest cavities observed on the propeller blades are not at the top position (12 o'clock) where the static pressure is the lowest, but at the bottom (6 o'clock) where the tunnel flow separates from the openings at the bottom. This is true both for the gear-driven system as well as for the rim-driven system.

The fact is that very often a thruster manufacturer has to design and provide the system without knowing all the details of the ship's hull and the tunnel openings which are often designed by the shipyards.

Strong gap flow at the gear-driven propeller tips and corner vortex cavitation at the root of the rim-driven ring-propeller have been observed, see Figure 15.

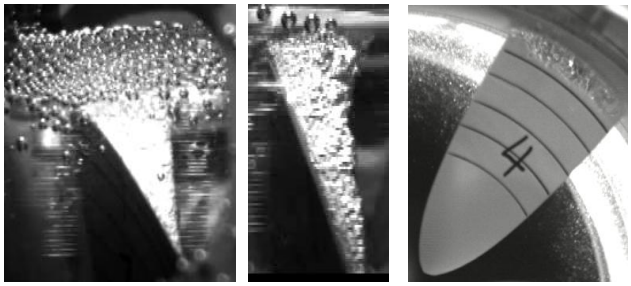

CTT1 FTT1 RFTT1

Figure 15 Tip flows (top view through tunnel wall, tunnel flow from right to left) of CTT1 and FTT1 (Kaplan, 4-bladed, constant pitch $P_{0.7R}/D_P$=0.9, BAR=0.6) and root corner flow (rotate CCW) of RFTT1 (5-bladed, $P_{0.7R}/D_P$= 0.9167, BAR=0.6), σ_n=2.5 at bollard.

Due to the increased pitch toward the tip of a planar CTT blade at a non-zero pitch, the tip flow of a CTT is stronger than that of an FTT at the same loading. The corner flow at the blade root of a rim-driven propeller is rather difficult to prevent from occurring. Careful design is necessary to prevent cavitation erosion at the blade root.

Forward skew has been said to reduce cavitation volume, vibration and noise levels of a tunnel thruster with planar blades of a CTT, due to the fact that the effective camber of the blade section at a non-zero pitch setting will be positive upstream the blade directrix and negative downstream the blade directrix, as illustrated in Figure 16 where the red lines are the directrix.

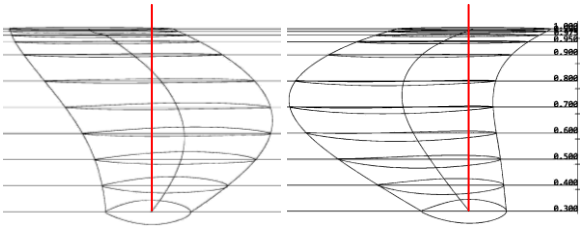

Figure 16 Effective camber of planar CTT blades at a non-zero pitch setting, left: CTT4 (highly-skewed, 4-bladed, $P_{0.7R}/D_P$=0.9, BAR=0.6); right: CTT3 (forward skewed, $P_{0.7R}/D_P$=0.9, BAR=0.6).

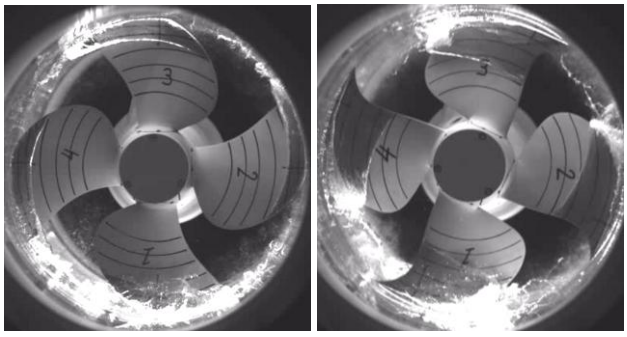

Figure 17 Left: CTT4, right: CTT3, σ_n=2.0, CW rotation.

However, designing CTT planar blades with complete strong forward skew for all radii of the blades is in most case not possible due to high spindle torque. A balanced skew is always necessary. Carefully choosing the skew distribution is essentially important for CTT planar blades, otherwise a seemingly forward-skewed blade, like CTT3 tested for the present project with negative effective camber, may result in larger cavity on the blades with higher vibration and noise levels (Figure 17).

FTT and RFTT propellers with zero camber, symmetric section profiles and identical leading and trailing edges on all radii of the blades operate far from the shock-free entry of the sections. Introducing a locally-cambered section profile at the leading edge, may reduce the suction peak and cavity size, such as an s-shaped chord-wise camber distribution with a zero mean, see Figure 18.

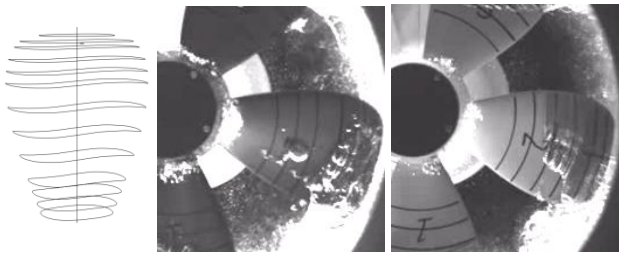

s-shaped camber FTT5 FTT3

Figure 18 Cavitation patterns observed on FTT5 (5-bladed, s-shaped camber, $P_{0.7R}/D_P$=0.9806 with tip/root unloading, BAR=0.6), compared to that on FTT3 (5-bladed, constant pitch $P_{0.7R}/D_P$=0.9, BAR=0.6), σ_n=1.5.

It can be clearly seen that an s-shaped chordwise camber distribution does reduce the cavity volume a lot, even at a very low cavitation number σ_n=1.5. As a consequence of it, the vibration and noise levels of such a propeller are expected to be lower. However, care has to be taken on the amount of local cambering with respect to operating conditions of the thruster so that no bubble cavitation should be present, as shown in the present study on FTT5 with local over-cambering for such a low cavitation number. Fine-tuning of s-shaped camber to obtain similar good performance as the tested one, but without bubble cavitation, may be investigated in the near future.

Different from a propeller designed as the main propulsion of a ship in its wake, blade tip and root unloading while keeping the same loading by increased pitch at the key radii, such as at 0.7R, may result in more cavitation in the mid of the blades, see Figure 19. The cavity planform may develop towards the tip in an unfavourable way. It has then a more 2D-like planform and may break-off in the mid of the blades and result in cavitation erosion.

6.2 Side force and efficiency

As the primary function of a tunnel thruster – generating side force on a ship's hull, the side force and the needed power input are measured and judged by the merit coefficient η_D. To understand and limit the Reynolds effects, tests were carried out in atmospheric condition at various rotation rates.

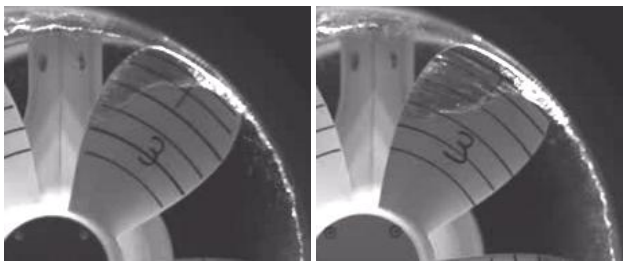

Figure 19 Left: FTT3, compared to, right: FTT4 (5-bladed, $P_{0.7R}/D_P$=0.9806 tip/root unloading, BAR= 0.6), σ_n=2.5.

Taken the 4 CTTs as example from 12 tested propellers, the propeller thrust T, torque Q and the gearbox pod thrust $F_{x\ pod}$, and the total side force on the hull $F_{x\ hull}$ are presented in Figure 20 at various rotation rates.

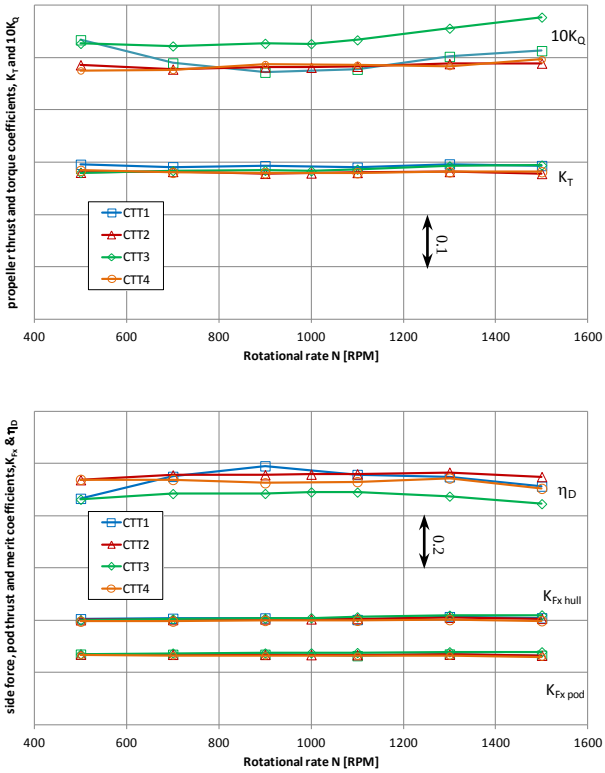

Figure 20 Comparison of the loads on CTT1, CTT2 (skewed, 4-bladed, BAR=0.6), CTT3 and CTT4 at the identical pitch setting of $P_{0.7R}/D_P$=+0.9, push mode.

Due to the fact that all CTTs have identical pitch setting at 0.7R with all planar blades, the thrust loadings of all CTTs are identical. This can be seen from the results of the propeller thrust T, the pod thrust $F_{x\ pod}$, and the total side force $F_{x\ hull}$. In addition, the thrust loadings are not sensitive to the Reynolds numbers as far as the rotation rate is higher than 500 RPM. However, the torque of the propellers is more sensitive to the Reynolds number. It is also found during the tests that the results are affected by small cavitation at the tip region when the rotation rate is very high, such as 1,500 RPM, even at atmospheric condition. The loads measured then do not represent a non-cavitating operation of the propeller in atmospheric condition any more.

Besides CTT3, which has a forwardly-skewed look, the other 3 CTTs have similar efficiency in generating the side force judged by their merit coefficients. However, due to the negative effective camber of the sections on their key radii, CTT3 is worse than the others by more than 5%.

To compare the performance of CTTs, FTTs and RFTTs with each other on the side force and efficiency, 4 typical propellers have been selected from 12 propellers tested in the initial investigations in this project and plotted in Figure 21.

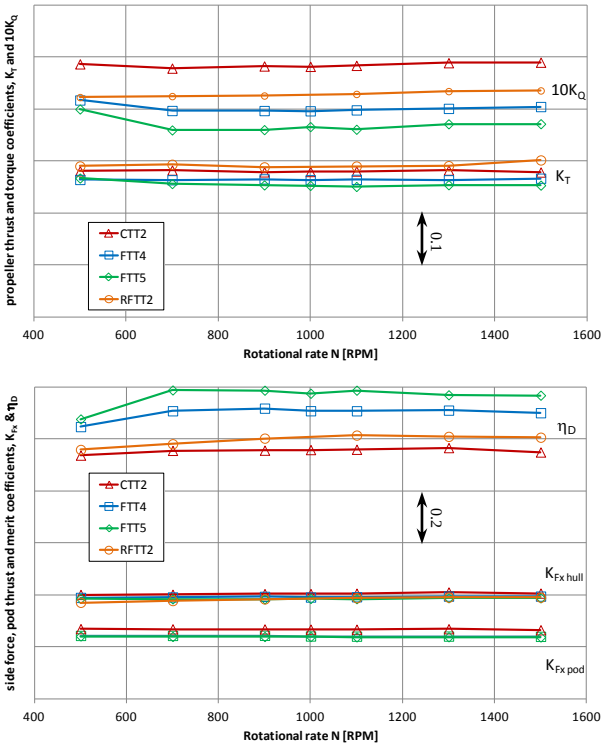

Figure 21 Performance comparison of CTT2, FTT4, FTT5 and RFTT2, gear-drive in push mode.

It can be seen in Figure 21 that the 4 selected propellers have slightly different propeller loadings on K_T, but they do not differ much on the total side force coefficients $K_{Fx\ hull}$, which are all on the same level. However, the propeller torque coefficients K_Q differ a lot, resulting in large efficiency difference on η_D. The FTTs have an η_D about 10% higher than that of the RFTTs, and the RFTTs have an η_D about 5% higher than that of the CTTs (which is about 15% lower than that of the FTTs). Such large systematic performance differences between CTTs and FTTs have never been reported from investigations in the past and no information on RFTTs was available in the public domain before.

However, it should be pointed out that the CTTs were tested with the same large gear-house as for the FTTs. When the gears are optimized for CTTs for one operation direction, the gear-house can be much smaller. This can improve the performance of CTTs. It should also be pointed out that the above comparison is not based on the same power. The large difference on the torque results in large power absorption difference for the cases.

Applying s-shaped section profiles to an FTT blade to improve cavitation performance has generated concerns if the efficiency of the thruster can be maintained as that of a conventional blade with symmetric sections without camber, because the local camber at the trailing edge was negative. However, the test results show that the performance of FTT5 with an s-shaped camber is equally good and even slightly better than that of FTT4.

6.3 Thrust breakdown

Due to the planar blades of CTTs and symmetric section profiles with identical leading and trailing edges of FTTs and RFTTs, high suction peaks will be always present at the leading edges of the blades, resulting in pre-mature or developed sheet cavitation. Therefore, tunnel thrusters are easier to run into a thrust breakdown situation during normal operations, than propellers of main propulsion systems. Industry surveys show that the majority of tunnel thrusters are operating in a range of rotational cavitation number σ_n from 1.5 to 2.5. In order to determine the thrust breakdown, tests by sweeping the rotation rate from 500 RPM to 1,500 RPM at 3 tank air pressure levels, plus also in the atmospheric condition, provides the performance covering a large range of cavitation numbers from non-cavitating condition to σ_n=1.5 or even lower. An example of a comparison between different types of blades is given in Figure 22.

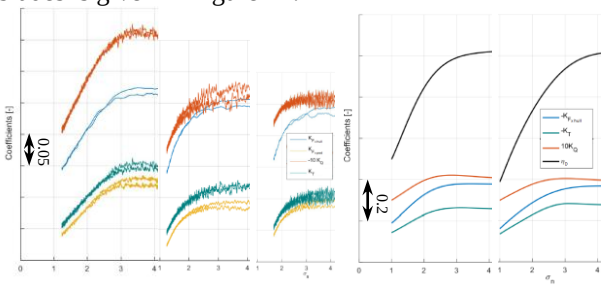

Figure 22 Comparison of thrust breakdown between CTT2, FTT4, FTT6 (7-bladed, $P_{0.7R}/D_P$=0.9806 tip/root unloading, BAR= 0.6) in push mode, and RFTT1 and RFTT2.

In Figure 22, the thrust breakdown results are plotted with the filtered raw data as measured during the RPM sweep tests for the selected gear-driven propellers (to show how the raw data look like), while the results of the rim-driven propellers are given by the polynomial fits (to show how the data is fitted). It should be pointed out that in all cases the thrust breakdown starts already from about σ_n=3.0. The breakdown seems to start even earlier for the 7-bladed from about σ_n=4.0, but gradually.

As the majority of tunnel thrusters are operating in a condition with a cavitation number σ_n between 1.5 to 2.5, it can be concluded that most tunnel thrusters are operating, in different degrees, in a thrust breakdown condition. Without understanding this, it may happen that the power absorption of a tunnel thruster is wrongly estimated in the design stage. It can be very much frustrating and costly if the pitch is wrong for FTTs or RFTTs, leading to propeller modifications. It implies also

that changing the draught of a ship (e.g. ballast to scantling) may affect the power absorption of a tunnel thruster by a lot.

6.4 Pressure fluctuations and tunnel excitations

With the pressure transducers fitted on the tunnel inner surface as shown in Figure 8, the pressure fluctuations on the tunnel inner surface were measured in all 3 cavitating conditions.

The pressure fluctuation levels were measured rather high in the vicinity of the propeller tips. An example is shown in Figure 23 for the model-scale measured values. Taken into account of the envisaged full-scale tunnel thruster with a scale ratio of 1:10, the values in full-scale will be 10 times larger than the values on model scale.

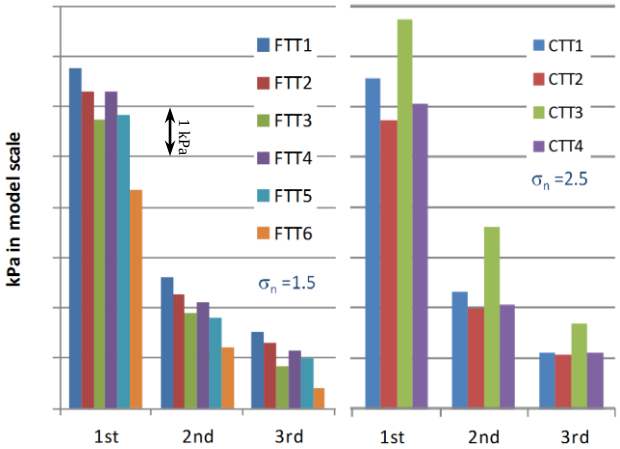

Figure 23 An example of comparing the highest pressure fluctuations of 30 pressure transducers measured in model scale for the first 3 blade passing frequencies, gear-driven, push mode, 1,000 RPM.

The test results clearly show that the pressure fluctuation levels reduce with the increase of the blade numbers, from FTT2 4-bladed to FTT3 5-bladed with both contemporary blade designs and constant pitch, and tested on equal thrust loadings, as well as from FTT4 5-bladed to FTT6 7-bladed with identical reduced root/tip loadings and also tested on equal thrust loadings.

The so-called 'forward-skewed' CTT3, resulting in more cavitation on the blades (see Figure 17), generates the highest pressure fluctuations in all 3 blade passing frequencies. Kaplan blades CTT1 is also slightly worse than the other modern designs CTT2 and CTT4.

Directly integrating the pressure fluctuations on the tunnel inner surface with phase differences to arrive at the tunnel excitation forces will face difficulties due to the high gradient of the phase variations and the standing waves in the tunnel. The excitation forces are hence directly measured by the 6C frame, as shown in Figure 6, on a tunnel segment.

The amplitudes of the vertical and horizontal excitation forces of the CTTs tested in the early stage of the project are shown in Figure 24 as an example, where the coefficients of the excitation amplitudes ΔK_{Fy} and ΔK_{Fz} are non-dimensionalised in the same way as Equation (2).

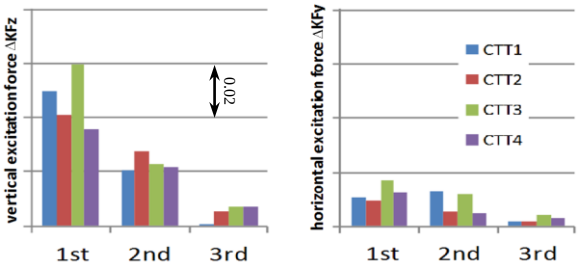

Figure 24 The single amplitudes of the vertical and horizontal excitation forces on the tunnel segment for the first 3 blade passing frequencies, σ_n=2.5, push mode, at 1,000 RPM.

Due to the fact that the largest cavitation volume was found on the propeller blades at the bottom of the tunnel (Figure 14) and that the cavity volume for the push mode is also large on the propeller blades at the top position when the blades are passing the wake of the gearbox strut, the collapse of the cavities at the top and bottom positions is the strongest, resulting in higher vertical tunnel excitations than that of the horizontal excitations.

However, it should be pointed out that only the amplitudes of blade passing frequencies of the measured values are reliable, the higher harmonics are only for indication. The following spectrum, in Figure 25, shows the natural frequencies of the tunnel segment model in the water during an RPM sweep test. Tunnel segment model resonance has already been found at about 100Hz.

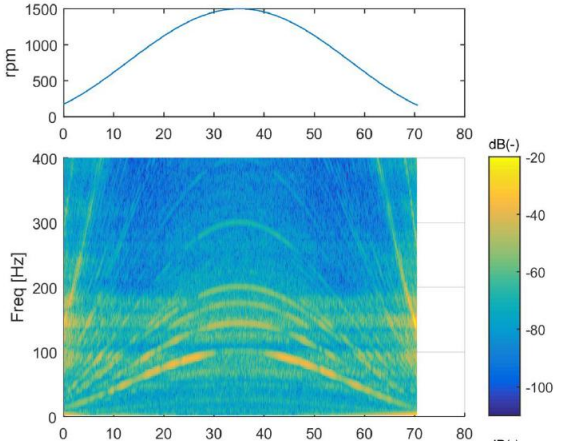

Figure 25 Spectrum of the tunnel vertical excitation force during an RPM sweep tests with CTT1 in non-cavitating condition.

6.5 Underwater radiated noise (URN) levels

To illustrate the test results for the underwater radiated noise (URN) levels and to make relative comparisons, the measured noise levels were converted to a distance of 1m from the source and plotted in Figure 26 for all 12 propeller models tested in the initial investigations of the project but at only one of the 3 cavitation numbers, one rotation direction and from one of the 3 hydrophones, together with the background noise levels.

Although the URN levels from the final TT-series propellers are provided as the noise source levels, corrected by the transfer functions, the presented results

in the figure are the receiving noise levels on model scale (not the source levels) in 1/3 octave band without corrections. Therefore, the model influence, the reflections and dissipation, the Lloyd's mirror effects, etc. are not corrected for. They are also not corrected for the frequency at full scale.

For CTTs, it won't be surprising that the noise levels of CTT3 with 'forwarded-skewed' blades have the highest noise levels after observing large cavitation on the blades (Figure 17), the CTT2 with contemporary blade design with medium and balanced skew has the lowest noise levels in the high frequency range, where cavitation noise is dominant.

Increasing the blade numbers seems to reduce the URN levels. This can be seen from the results of the FTTs. FTT6 with 7 blades seems to have the lowest noise levels in the high frequency range of all FTTs tested.

Generally speaking, the FTTs have higher underwater radiated noise levels than that of the CTTs, by about 10dB. This could be linked to the fact that cavitation on the FTTs is generally less stable than that on CTTs, with the propeller FTT5 with s-shaped camber as the worst with unstable bubbly cavitation on the blades.

Obviously, the lowest underwater radiated noise receiving levels were measured for the RFTTs. However, this does not indicate the source level difference because the transfer function for the rim-driven system is different from that of the gear-driven system.

7 CONCLUDING REMARKS

After the initial investigation on the design strategy of tunnel thruster propeller blades used to generate side force to either direction (starboard or portside), the Wageningen TT-Series Propellers have been established, which consists of 3 CTTs of 4 blades at various pitch settings, 24 FTTs of various BAR and design pitch ratios for 3 blade numbers (4, 5 and 7), and 9 RFTTs with limited variations on blade numbers, BAR and pitch ratios, considering a practical rim-drive system.

All propellers of the series have been tested for their side force performance as well as the static and dynamic loads. Selected propellers have been tested for cavitation, pressure fluctuations, tunnel excitation forces, and underwater radiated noise (URN) levels, including also cavitation-induced thrust breakdown. Together with the investigations on the TT-series propellers in various tunnel and hull forms and the effects of the wall inclinations, the tunnel length and entrance forms, the grid bars, and the pod supports, all aspects of the above mentioned tunnel thruster performance for the whole series are obtained by interpolations.

The series form important databases for tunnel thruster selections/designs, performance estimations and CFD validations. Software has been developed on the basis of the databases with interpolations that has three major functions: the selection and design, the prediction and scenario analyses of the selected solution, and the final generation of the propeller geometry from the series when satisfied with the performance of the selected solution.

The Wageningen TT-Series Propellers are the first sets of its kind for the industry, not only to determine the side force on the ships' hull, but also to estimate the vibration and noise levels generated by a tunnel thruster. It is highly possible that the series, developed together with many industry partners (listed and acknowledged is this paper), will become the new industry standard in the very near future.

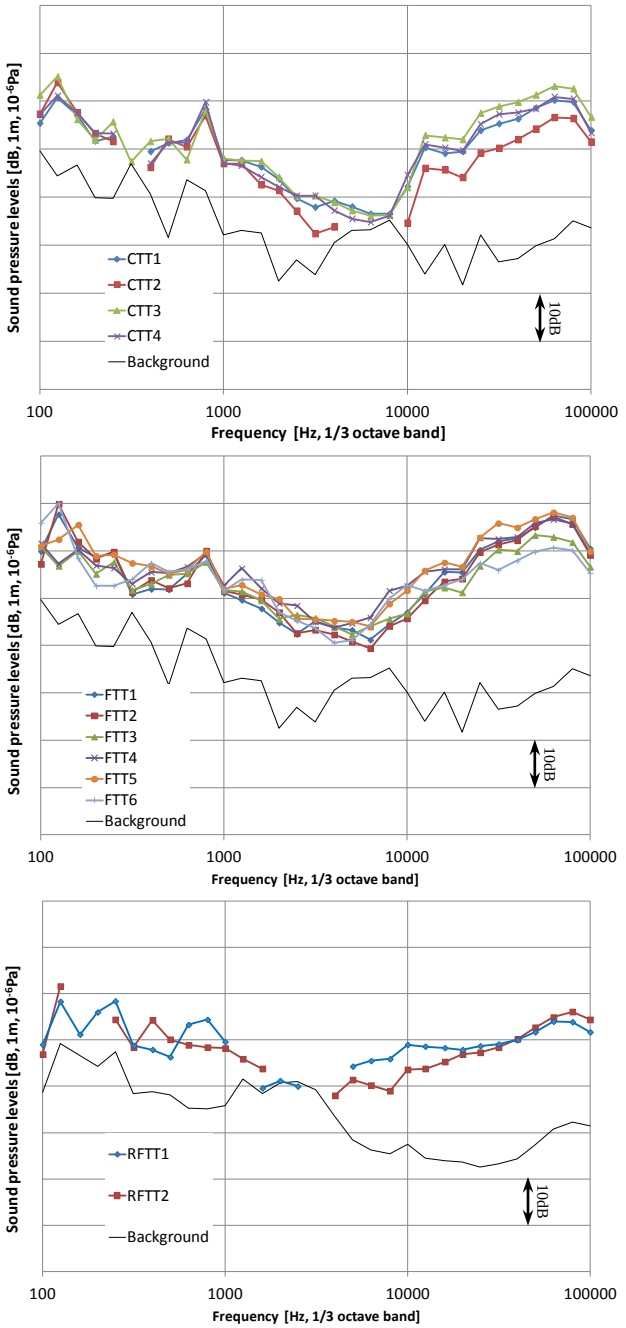

Figure 26 Underwater radiated noise (URN) receiving levels in model scale, un-corrected, from hydrophone No. 3 beneath the ship segment model with 65° inclined walls, σ_n=2.5, push mode for the gear-drive, at 1,000RPM for the gear-driven system and 900 RPM for the rim-driven system.

ACKNOWLEDGEMENTS

The authors thank all participants in the Joint Industry Project of Wageningen TT-Series Propellers: Advance Gearbox, Brunvoll, Caterpillar, CMDRC, CSSRC, Damen, Fincantieri-CETENA, IHC, Jastram, Kamome, Kawasaki, MARIC, MARIN, Nakashima, Navantia, NGC, Oceanco, Rolls-Royce, Scana Volda (merged with Brunvoll), Schottel, SMERI, SMMC, Voith and Wärtsilä. In addition, this JIP has also been supported by MARIN's research fund MaFu and Dutch government TKI funding. Thanks also go to all MARIN colleagues who were involved in this project with brilliant ideas on the test set-ups, the transducers and the data analyses.

REFERENCES

Beveridge, J.L., (1971) 'Design and performance of bow thrusters', NSRDC Report No. 3611, September.

Brix, J.E. and Bussemaker, O., (1973) 'Lateral thrusters with anti-suction tunnels', Proceedings 1st International American Tug Convention, Vancouver B.C., Canada, October.

Buiten, J. and Regt, M.J.A.M de, (1983) 'Handboek voor de lawaaibeheersing aan boord van schepen' (in Dutch), TPD report No. 208.431, Delft, The Netherlands, October.

Carlton J. (2007) 'Marine Propellers and Propulsion, Second Edition', Elsevier ISBN: 978-07506-8150-6.

Chislett, M.S. and Björheden, O., (1966) 'Influence of ship speed on the effectiveness of a lateral-thrust unit', Hydro- og Aerodynamisk Laboratorium Lyngby, Denmark, Report No. Hy-8, April.

Dang, J., Koning J., Brouwer J. and de Jong J., (2013) 'Dynamic Loads on Mechanical Azimuthing Thrusters', Proceedings of the PRADS2013, 20-25 Oct. CECO, Changwon City, Korea.

Dang, J., (2014) 'DP Thrusters – Understanding Dynamic Loads and Preventing Mechanical Damages', Proceedings of Dynamic Positioning Conference, Houston, October.

Dang, J. and Brouwer, J. (2015) 'External Hydrodynamic Loads on the Shaft of Azimuthing Thrusters and Podded Propulsors', Proceedings of Propeller & Shafting Symposium, Virginia Beach, September.

English, J. W. (1963) 'The Design and Performance of Lateral Thrust Units for Ships, Hydrodynamic Considerations', Transactions of RINA.

Funeno, I., (2006) 'Analysis of Hydrodynamic Forces on a Propeller Blade of Tunnel Thrusters in Bollard Conditions', Proceedings of 2nd PAAMES and AMEC2006, Jeju Island, Korea.

Kijima, K., (1977) 'The effect of drift angle on side thrusters performance', Transactions of the West-Japan Society of Naval Architecture, 54.

Klinkenberg, Y., Bosman, R., Dang, J. and Ligtelijn, J. Th., (2017) 'Advanced Measurements of RIM-driven Tunnel Thrusters', Proceedings of the 5th International Conference on Advanced Model Measurement Technology for the Maritime Industry (AMT'17), Glasgow UK, October.

Ligtelijn, J.T. and Otto, R., (2013) 'Minimization of noise and vibrations from transverse propulsion units', 2nd IMAREST Ship Noise and Vibration Conference, London, U.K.

Mohan, A., (2017) 'Numerical Analysis of Bow Tunnel Thruster Performance', Master of Science Thesis, Delft Technical University.

Nienhuis, U., (1992) 'Analysis of thrusters effectivity for dynamic positioning and low speed manouvering', PhD Thesis, Delft University, The Netherlands.

Pehrsson, L., (1960) 'Model tests with bow-jet (bow-steering) screw propellers', First Symposium on Ship Manoeuvrability", pp25–48, David Taylor Research Centre.

Pronk, C. and Schneiders, C.C., (1976) 'Propulsion for offshore vessels', 3rd Lips Propeller Symposium, Drunen, The Netherlands, May.

Taniguchi, K., Watanabe, K. and Kasai, H., (1966) 'Investigations into the fundamental characteristics and operating performances of side thrusters', Mitsubishi Technical Bulletin No.35, May.

Verbeek, R., (1982) 'De netto stuwkracht van thrusters' (in Dutch), Lips Technical Report 5330-8201, March, written for the Dutch organisation CMO under contract 81/1693/7.3.